SCIENCE CHINA Materials ARTICLES

mater.scichina.com link.springer.com

Published online 20 May 2021 | https://doi.org/10.1007/s40843-021-1664-0
Sci China Mater 2021, 64(11): 2805–2812

Full-color flexible laser displays based on random laser arrays

Yue Hou[1,2], Zhonghao Zhou[1], Chunhuan Zhang[1], Ji Tang[1], Yuqing Fan[1,2], Fa-Feng Xu[1] and Yong Sheng Zhao[1,2*]

ABSTRACT **Flexible laser display is a critical component for an information output port in next-generation wearable devices. So far, the lack of appropriate display panels capable of providing sustained operation under rigorous mechanical conditions impedes the development of flexible laser displays with high reliability. Owing to the multiple scattering feedback mechanism, random lasers render high mechanical flexibility to withstand deformation, thus making them promising candidates for flexible display planes. However, the inability to obtain pixelated random laser arrays with highly ordered emissive geometries hinders the application of flexible laser displays in the wearable device. Here, for the first time, we demonstrate a mass fabrication strategy of full-color random laser arrays for flexible display panels. The feedback closed loops can be easily fulfilled in the pixels by multiple scatterings to generate durative random lasing. Due to the sustained operation of random laser, the display performance was well-maintained under mechanical deformations, and as a result, a flexible laser display panel was achieved. Our finding will provide a guidance for the development of flexible laser displays and laser illumination devices.**

Keywords: perovskite nanocrystals, random laser, microlaser arrays, flexible displays, laser displays

INTRODUCTION

Benefiting from the intense coherent emission across full visible spectrum, laser-based displays have great potential for revolutionizing the traditional display technologies due to their wide gamut range, high contrast ratio and excellent color saturation [1–3]. The ever-increasing demands on laser displays in portable and wearable devices call for self-emissive flexible display panels, which can withstand mechanical deformation [4–8]. Integrating red, green, and blue microlasers into periodic arrays on flexible polymer substrates is an effective solution to fabricate flexible display panels [9–15], which can be mechanically bent or stretched without compromising their laser performance. However, the traditional resonant cavities could be easily damaged under mechanical deformation, making it challenging to realize such a flexible lasing device [16–21].

Random lasers characterized with easy fabrication and flexibility, which can be ascribed to their multiple scattering mechanisms to provide optical feedback [22–23], are promising candidates to construct flexible laser display panels [24–25]. Moreover, the emission of random lasers exhibits the wide angular distribution, making them ideal illuminants for broad-view-angle display [26–28]. To this end, precisely patterning random lasers into well-arranged red-green-blue (RGB) arrays is highly desired for the implementation of full-color flexible laser display panels [29–31]. Various methods have been proposed for the fabrication of random lasers, such as spin-coating, chemical vapor deposition and drop-casting [32–35]. However, the acquisition of full-color random laser arrays with these methods has been hindered by the difficulties in precisely patterning RGB random laser arrays with highly ordered emissive geometries. Therefore, developing a feasible and general technique to finely pattern random lasers into pixelated microlaser arrays would represent a step toward the acquisition of full-color panels for flexible laser displays.

Herein, we propose a universal strategy to fabricate pixelated random laser arrays *via* the microtemplate-assisted inkjet printing for flexible full-color laser display panels. Owing to their tunable bandgap, large optical gain, and solution processability, perovskite nanocrystals

[1] Key Laboratory of Photochemistry, Institute of Chemistry, Chinese Academy of Sciences, Beijing 100190, China
[2] University of Chinese Academy of Sciences, Beijing 100049, China
* Corresponding author (email: yszhao@iccas.ac.cn)

(Pe-NCs) with different halide anions were selected as gain materials to construct red, green, and blue-emissive microlasers. The microlasers were precisely positioned by flexible polymeric microtemplates to acquire ordered arrays with well-organized geometry. Appropriately exciting each of the three adjacent microstructures enabled full-color tunable lasing to build an individual RGB display pixel. On this basis, we have achieved full-color flexible laser display panels with the RGB microlaser arrays. Moreover, the flexibility and broad angular emission of random lasers in the pixels enable the display device to exhibit stable performance under deformation. The random laser arrays with outstanding mechanical performance as display panels will support the innovation of concepts and device architectures in portable and wearable devices.

EXPERIMENTAL SECTION

Fabrication of Pe-NCs random laser arrays

The silicon mother-molds were cleaned using oxygen plasma for 5 min to produce hydrophilic surfaces. Then, a thin layer of 1H,1H,2H,2H-perflfluorooctyltriethoxysilane was coated on the substrate surface to induce a hydrophobic effect. The polydimethylsiloxane (PDMS)-microtemplates were fabricated by casting PDMS against a silicon mother-mold consisting of convex cylinder arrays. The synthesis methods of Pe-NCs/SiO_2 were modified according to previous literature (see more details in Supplementary information) [36]. Pe-NCs/SiO_2 composites (100 mg mL^{-1}) were dispersed in a mixture of toluene and 1-octadecene (3:1). Then, the Pe-NCs/SiO_2 composite solutions were imbibed into a hollow glass needle *via* the capillary effect and accurately injected into these blank microtemplates. After drying in air for 20 min, random laser arrays were obtained.

Morphological characterization

The morphologies of the polymeric microtemplates were examined by a step profiler (Bruker Dektak XT) and a contourgraph (Bruker Contour GT-K1). The morphologies of the random laser arrays were examined by scanning electron microscopy (SEM, Hitachi SU8010). The size distribution of Pe-NCs/SiO_2 was characterized by transmission electron microscopy (TEM, JEOL 2100).

Optical characterization of individual microlaser

The transmission and fluorescence spectra were measured by an ultraviolet (UV)-visible spectrometer (Perkin-Elmer Lambda 35) and a fluorescent spectrometer (Hitachi F-7000), respectively. Bright-field and fluorescence microscopy images were acquired using an inverted fluorescence microscope (Nikon Ti-U) by exciting the samples with the halogen and mercury lamps, respectively. The optically pumped lasing measurements for individual pixels were carried out on a custom microphotoluminescence system. The excitation pulses (400 nm) were generated from the second harmonic of the fundamental output of a regenerative amplifier (Spectra Physics, 800 nm, 150 fs, 1 kHz), which was in turn seeded by a mode-locked Ti: sapphire laser (Mai Tai, Spectra Physics, 800 nm, 150 fs, 80 MHz). The excitation laser was filtered with a 720-nm short-pass filter and then focused down to a spot through an objective lens (Nikon CFLU Plan, ×10, N.A. = 0.3) as a nearly uniform pump source. The power at the input was altered by a neutral density filter. The emissions from the individual microstructure were collected by the same objective with a back-scattering configuration and analyzed by the spectrometer after removal of the excitation beam with a 420-nm long-pass filter.

Angle-resolved photoluminescence (ARPL) measurements of individual microlasers

The incident light (400-nm femtosecond laser) was focused onto the random laser arrays by a microscope objective (Nikon CFLU Plan, 100×, N.A. = 0.8). The PL of the microstructures was focused at the rear focal plane of the same objective, which was then projected onto the entrance slit of a spectrometer equipped with a charge-coupled device (CCD). Therefore, the two orthogonal axes of the CCD correspond to the wavelength λ (equivalently as energy, E) and angle θ (equivalently as wave vector, k) of the detected light, respectively.

RESULTS AND DISCUSSION

Fig. 1a shows the design concept of flexible laser display based on the controllable integration of RGB random laser pixel arrays. Display pixels with well-organized geometry could be achieved *via* a solution processing method. In these individual pixels, monodisperse silica spheres serve as the scatter medium to provide optical feedback, and Pe-NCs attached to the surfaces of spheres act as the gain materials. Benefiting from the multiple scattering feedback mechanism of random laser, the optical feedback can be easily fulfilled in the pixel even under mechanical deformation, which is crucial for the stable operation of lasing with flexibility (Fig. 1a, bottom). Accordingly, three kinds of Pe-NCs, including $CsPbCl_{1.5}Br_{1.5}$, $CsPbBr_3$ and $CsPbBrI_2$ with emission from

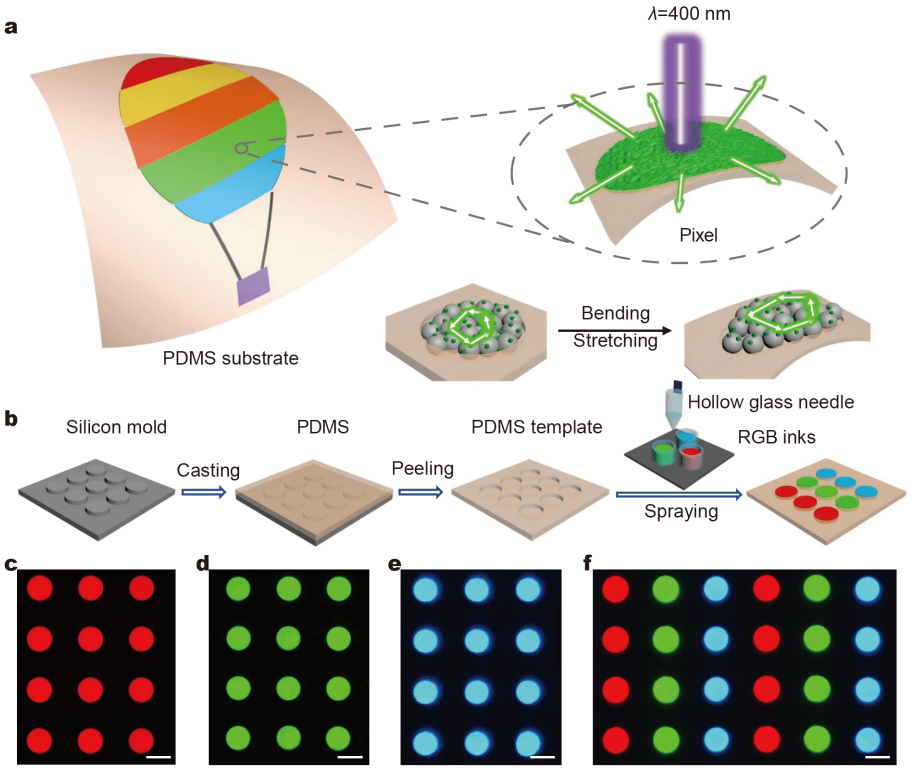

Figure 1 Design and fabrication of the flexible random laser arrays. (a) Design principle of the flexible laser display based on random lasers. (b) Schematic illustration for the fabrication of periodic RGB pixel arrays *via* microtemplate-assisted inkjet printing. (c–f) Fluorescence microscopy images of the periodic pixel arrays comprising red, green, blue and RGB emissive arrays under UV light radiation (330–380 nm). All scale bars are 50 μm.

blue to red (Fig. S1), were selected as model materials to construct RGB random lasers due to their high optical gain and facile solution processibility [37–41]. Monodisperse silica spheres were applied as scattering media for optical feedback (Fig. S2). The Pe-NCs uniformly adhered on the monodisperse silica spheres *via* chemical modification (Fig. S3), which was demonstrated to depress the optical degradation of PL effectively for enhancing random lasing stabilities [36].

The random laser arrays were prepared by selectively printing the droplets of Pe-NCs/SiO_2 ink solution at specific positions on PDMS substrates according to the predesigned digital patterns (Fig. 1b). First, the PDMS template was fabricated by casting PDMS against a silicon mother-mold with circularly microtemplate convex. After curing, the PDMS template was detached from the silicon mold and served as blank microtemplates. The as-fabricated soft microstructures were highly uniform (Fig. S4) with dense packing density. These microtemplates with depth of 10 μm (Fig. S5) can accommodate the active material to provide sufficient optical gain for stimulated emission. Then, the ink solutions of Pe-NCs/SiO_2 composites were imbibed into a hollow glass needle *via* the capillary effect and accurately injected into the blank microtemplates by ultrasonic vibration. The SEM images in Fig. S6 show that the composites are full-filled in the blank microtemplates, which is crucial for the uniform emission from the pixels. The fluorescence optical microscopy images (Fig. 1c–e) manifest that the red, green, and blue arrays are patterned over a large area with a uniform geometric shape. The sizes of the microstructures were modulated rationally by varying the corresponding structure parameters of the microtemplates (Fig. S7). Benefiting from the precise positioning of inkjet printing, we have prepared an RGB pixel array (Fig. 1f), showing the feasibility of the printed RGB arrays as full-color self-emissive laser display panels.

A homebuilt far-field microphotoluminescence system was used to perform optically pumped lasing measurements of the microstructures (Fig. S8). The Pe-NCs/SiO_2 microstructures were uniformly excited with a pulsed laser beam (400 nm, 150 fs, 1 kHz) and the spectral evolutions with increasing pump power are shown in Fig. 2a–c. At low pump energies with fluence

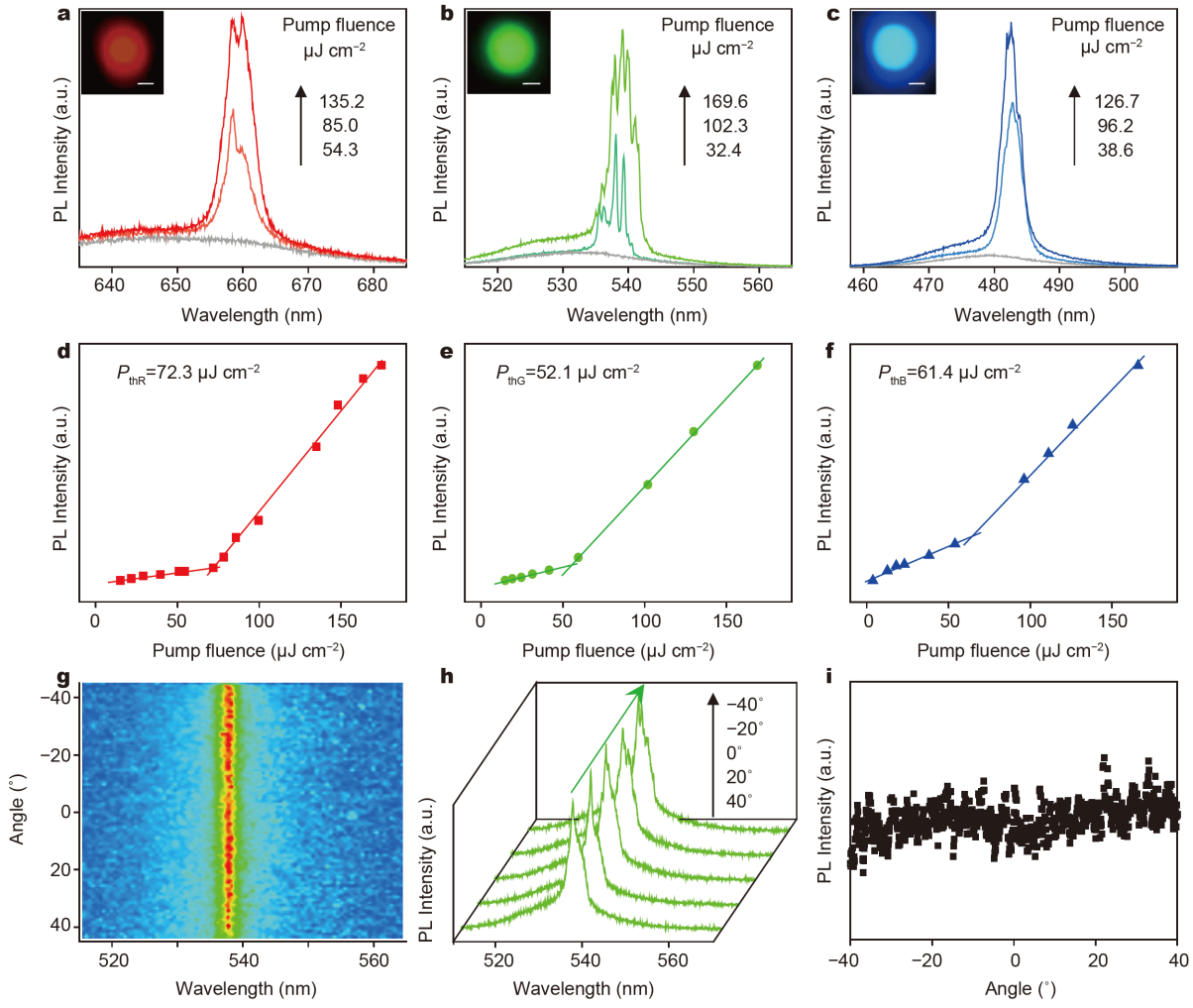

Figure 2 RGB random lasing of an individual pixel. PL spectra from an individual pixel under different pump fluences with excitation on the (a) red-emissive microstructure, (b) green-emissive microstructure, and (c) blue-emissive microstructure, respectively. Insets: corresponding microscopy images of the RGB lasing microstructures. All scale bars are 20 μm. (d–f) Plots of the PL peak intensities at 658, 536, and 483 nm *vs.* pump fluence, showing the lasing thresholds of 72.3, 52.1, and 61.4 μJ cm^{-2}, respectively. (g) Far-field ARPL emission spectrum mappings of green-emissive microstructures at 52.1 μJ cm^{-2}. (h) Lasing spectra and (i) lasing intensity at 536 nm of green-emissive microstructure at different angles.

<51.2 μJ cm^{-2}, all PL spectra were dominated by broad spontaneous emissions. With increasing pump fluence, strong laser emissions developed as a set of sharp peaks of red, green, and blue centered at 658, 536, and 483 nm, respectively. The plots of the corresponding lasing intensities as a function of pump fluence exhibit clear knee characteristics (Fig. 2d–f), further confirming the lasing action from the printed RGB emissive microstructures. At a higher optical pumping energy density above the lasing threshold, multiple lasing peaks occur, which is one of the typical characteristics of the random lasing action [28,42]. Owing to the multiple scattering mechanism for trapping light, the random lasers in our system exhibit low spatial coherence (Fig. S9). Moreover, sustained operation of the random laser was achieved after scanning 1×10^6 times (Fig. S10), showing their potential in serving as robust self-emissive laser display pixels.

ARPL measurements were examined to elucidate the characteristics of broad angular distribution of the random lasing in these RGB microstructures (Fig. S11). A large-angle (0°–52°) radiation of the lasing mode is observed in the green subpixels (Fig. 2g), which should be attributed to the random scattering of the microspheres (Fig. S12, for blue subpixels and red subpixels). The resonance modes of the cavity accorded with multiple scattering feedback mechanism, which is inconsistent

with the whispering-gallery-mode (WGM) and Fabry-Pérot (F-P) theory (Fig. S13). Emission spectra above the threshold at the detection angles of −40°, −20°, 0°, 20° and 40° were extracted, and the shapes of these lasing peaks remain almost unchanged (Fig. 2h). The variation of lasing intensities with detection angles is negligible (Fig. 2i), which is promising for stable display performance under deformation.

The multicolor lasing behavior of the microstructures provides an opportunity to construct full-color pixelated panels for laser displays through additive color mixing. Here, we evaluated the color expression based on the emission spectra of several subpixel combinations by selectively exciting the adjacent two or three microlasers in a single pixel (Fig. 3a). When the excitation beam was focused on the microstructure doped with $CsPbCl_{1.5}Br_{1.5}$, lasing at ~482 nm occurred, and a blue spot was observed in the RGB pixel. As the excitation beam was manipulated to irradiate on the microstructures doped with $CsPbBr_3$ (or $CsPbBrI_2$), the spectra were dominated by green or red (G or R) emission induced by lasing. When the blue- and green-emissive microstructures were simultaneously pumped above thresholds, two-color lasing (blue + green, B + G) was obtained. By adjusting the manner of excitation, any light combination in varying proportions can be generated, such as yellow (G + R), magenta (B + R) and white (B + G + R). Fig. S14, Tables S1 and S2 show the International Commission on Illumination (CIE) color diagram of the calculated chromaticity for these lasing spectra, and the chromaticity of the balanced white lasing (B + G + R) is very close to that of the CIE standard white illuminant D65 [43]. In addition, according to Grassmann's law, mixing the three primary colors in appropriate proportions can get all colors inside the triangle defined. Compared with the standard RGB space, the printed RGB pixel can cover 17.8% more perceptible colors, which suggests superiority of the random laser arrays in the production of vivid displays with excellent color saturation.

Accurate color rendering in the far-field was further examined by taking real color photographs of pixelated laser arrays with a built-in digital camera in a cell phone under laser irradiation [44]. The "ICCAS" pattern composed by a series of microlaser arrays was fabricated by selectively printing Pe-NCs/SiO_2 inks on a flexible substrate. As depicted in Fig. 3b, not only red, green, and blue "ICCAS" patterns comprising the printed monochromatic microstructures but also cyan, yellow, and magenta patterns composed of B + G, G + R, and B + R emissive microstructures, respectively, were obtained in

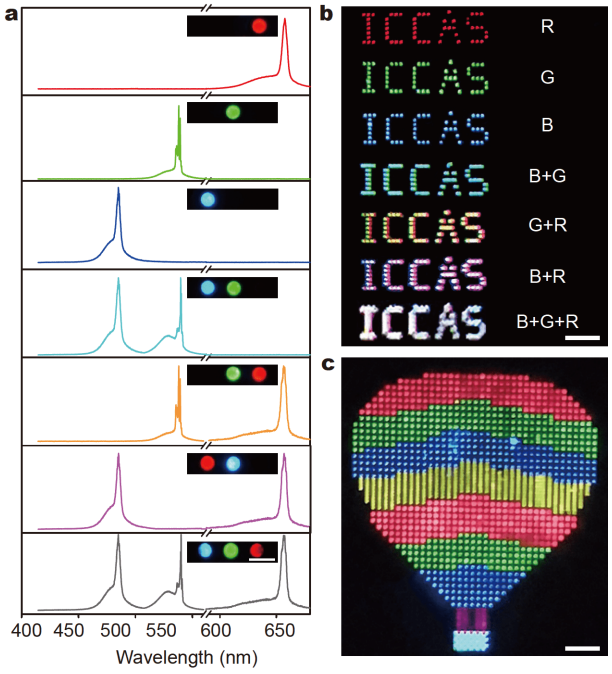

Figure 3 Full-color tunable lasing. (a) Lasing spectra and corresponding PL images while selectively exciting the different microlasers above their thresholds. From top to bottom: R, G, B, B + G, G + R, B + R, and B + G + R emissive microstructures. The scale bar is 100 μm. (b) Far-field photograph of the "ICCAS" patterns of pixel arrays comprising different microlasers, showing R, G, B, B + G, G + R, B + R, and B + G + R lasing emission, respectively. The scale bar is 800 μm. (c) Far-field photograph of a hot air balloon pattern with a 40 × 44 pixel array on a PDMS substrate. The scale bar is 700 μm.

the far-field and captured readily by naked eyes. Furthermore, a rendered white-emissive pattern was acquired when the RGB microlaser array was exploited. Laser displays can be realized on the printed RGB pixel arrays by controllably lighting up pixels in different locations as any image can be viewed as a matrix of pixels (Fig. S15) [45]. A large-scale image pattern was successfully realized by predesigning the patterned RGB microlaser arrays with distinct color emission at special positions on a substrate. Encouraged by the excellent performance of photographs of patterned multicolor microlaser arrays, we further achieved a hot-air balloon pattern based on such a 40 × 44 pixel RGB microlaser array on a flexible substrate in Fig. 3c, which manifests the applicability of the random laser arrays as self-emissive full-color panels for flexible laser displays. The broad-view-angle display performance of the panels was evaluated by testing the image quality from different view-angles. Clear hot-air balloon patterns were observed form ~0°, 30° and 60° (Fig. S16), implying the potential of

the printed display panel for broad-view-angle display.

The operational stability of laser under mechanical deformation, as a crucial issue in the design of flexible laser displays, was measured by deforming the pixels of the panels with a mechanical experimental setup (Fig. S17). Fig. 4a, b show the lasing intensity of the RGB laser under various strains ($\varepsilon = \Delta L/L_0$, L_0 is the initial length and L is the length after stretching. The values of strains were from 0 to 50%) and curvatures ($c = 1/\rho$, ρ is the bending radius of the PDMS substrate). The values of curvatures were from 0 to 0.12 mm^{-1} with a fixed pump fluence of 115.7 $\mu J\ cm^{-2}$. The lasing intensity changed within a small range beyond the naked eye recognition, which is crucial for realizing stretchable display. Meanwhile, the negligible variations of wavelengths and lasing thresholds under stretching and bending further confirm the mechanical stability of the random laser (Figs S18–S20). The distinct stability of laser operation should be attributed to the strong multiple scatterings in the pixels, which offers sufficient optical feedback for the gain to overcome loss. The lasing thresholds of the device were almost unchanged after 100 cycles with 50% stretching and a curvature of 0.12 mm^{-1} (Figs S21 and S22), which shows the outstanding reliability of the device under stretching. These results demonstrate that the random lasers with excellent mechanical properties are optimal light source for fabricating flexible laser display panels.

We demonstrated the display performance of the flexible laser display panels by controllably stretching and bending as illustrated in Fig. 4c. The stretched device shows uniform and bright emission across the entire luminous area, even when the device is stretched up to 60% strain (Fig. 4d). The almost unchanged display performance after tens of continuous cycles demonstrates the outstanding stability and reliability of the device. In order to further explore the potential of the random laser arrays to implement in flexible display, a severe bending test was carried out. Fig. 4e shows a stable operation of the random laser device with curvature up to 0.129 mm^{-1}. The

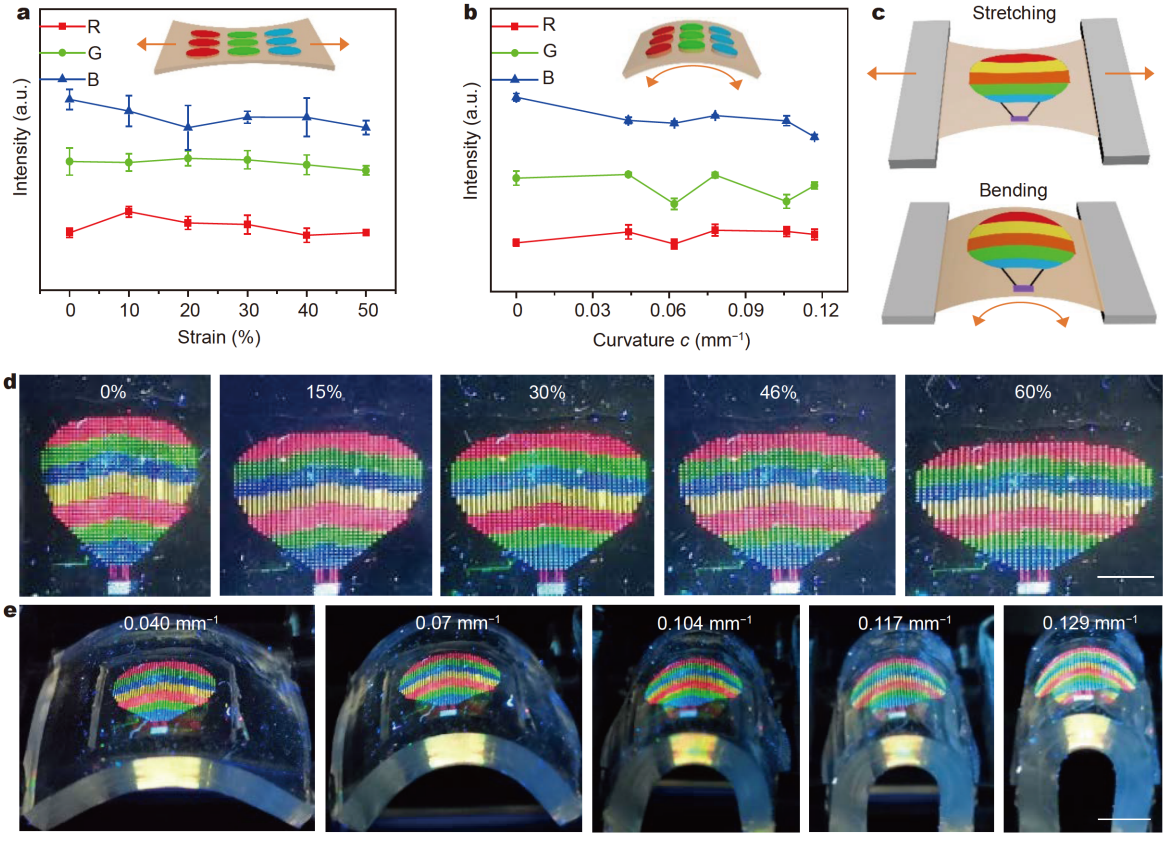

Figure 4 Demonstration of the flexible full-color laser display. (a) Plots of lasing intensities of an identical pixel at 658, 536, and 483 nm *vs.* strain values. (b) Plots of the lasing intensities of an identical pixel at 658, 536, and 483 nm *vs.* curvature (mm^{-1}). (c) Schematic illustration of the display performances of the flexible panel under stretching and bending. (d) Digital photographs of intrinsically stretchable multipixel display under different strains. The scale bar is 2 mm. (e) Digital photographs of multipixel display under different curvatures. The scale bar is 4 mm.

flexible laser display panel is also subjected to repeated cycles of bend and relaxation. Moreover, the device can continue to work under twisting conditions (Fig. S23), which verifies the high flexibility of the device. These prototypes demonstrate that the flexible panels formed by pixelated random microlaser arrays under deformation exhibit excellent display performance, which are applicable to wearable devices.

CONCLUSIONS

In conclusion, we have developed a universal strategy for constructing flexible full-color laser display panels with RGB microlaser arrays through a microtemplate-assisted inkjet printing method. Pe-NC microlasers were well positioned into an RGB pixel matrix according to the geometry of the microtemplates, where each set of adjacent RGB microlasers constituted an individual display pixel. The output of a single RGB pixel was tuned over a wide range of visible color *via* controlled pumping, thereby facilitating accurate color rendering in the far-field. Moreover, the microlaser pixels can be stretched by up to 60% and bended by up to 0.12 mm^{-1}, which makes the device flexible, bendable, and wearable. These results provide inspiration for the construction of flexible multicolor laser arrays and open new avenues for creating high-performance wearable laser display and lighting devices.

Received 1 February 2021; accepted 11 March 2021; published online 20 May 2021

1 Zhao J, Yan Y, Gao Z, *et al.* Full-color laser displays based on organic printed microlaser arrays. Nat Commun, 2019, 10: 870
2 Chellappan KV, Erden E, Urey H. Laser-based displays: a review. Appl Opt, 2010, 49: F79
3 Zhou Z, Zhao J, Du Y, *et al.* Organic printed core-shell heterostructure arrays: a universal approach to all-color laser display panels. Angew Chem Int Ed, 2020, 59: 11814–11818
4 Park SI, Xiong Y, Kim RH, *et al.* Printed assemblies of inorganic light-emitting diodes for deformable and semitransparent displays. Science, 2009, 325: 977–981
5 Yokota T, Zalar P, Kaltenbrunner M, *et al.* Ultraflexible organic photonic skin. Sci Adv, 2016, 2: e1501856
6 Liang J, Li L, Niu X, *et al.* Elastomeric polymer light-emitting devices and displays. Nat Photon, 2013, 7: 817–824
7 White MS, Kaltenbrunner M, Głowacki ED, *et al.* Ultrathin, highly flexible and stretchable PLEDs. Nat Photon, 2013, 7: 811–816
8 Choi M, Bae SR, Hu L, *et al.* Full-color active-matrix organic light-emitting diode display on human skin based on a large-area MoS_2 backplane. Sci Adv, 2020, 6: eabb5898
9 Choi MK, Yang J, Kang K, *et al.* Wearable red–green–blue quantum dot light-emitting diode array using high-resolution intaglio transfer printing. Nat Commun, 2015, 6: 7149
10 Kim TH, Cho KS, Lee EK, *et al.* Full-colour quantum dot displays fabricated by transfer printing. Nat Photon, 2011, 5: 176–182
11 Zhong Y, Liao K, Du W, *et al.* Large-scale thin $CsPbBr_3$ single-crystal film grown on sapphire *via* chemical vapor deposition: Toward laser array application. ACS Nano, 2020, 14: 15605–15615
12 Gao R, Zhao M, Guan Y, *et al.* Ordered and flexible lanthanide complex thin films showing up-conversion and color-tunable luminescence. J Mater Chem C, 2014, 2: 9579–9586
13 Liang J, Chu M, Zhou Z, *et al.* Optically pumped lasing in microscale light-emitting electrochemical cell arrays for multicolor displays. Nano Lett, 2020, 20: 7116–7122
14 Shi L, Meng L, Jiang F, *et al. In situ* inkjet printing strategy for fabricating perovskite quantum dot patterns. Adv Funct Mater, 2019, 29: 1903648
15 Fang X, Yang X, Li D, *et al.* Modification of π–π interaction and charge transfer in ratiometric cocrystals: Amplified spontaneous emission and near-infrared luminescence. Cryst Growth Des, 2018, 18: 6470–6476
16 Cloutier SG, Kossyrev PA, Xu J. Optical gain and stimulated emission in periodic nanopatterned crystalline silicon. Nat Mater, 2005, 4: 887–891
17 Chen R, Tran TTD, Ng KW, *et al.* Nanolasers grown on silicon. Nat Photon, 2011, 5: 170–175
18 Zhang C, Zou CL, Dong H, *et al.* Dual-color single-mode lasing in axially coupled organic nanowire resonators. Sci Adv, 2017, 3: e1700225
19 Dong H, Zhang C, Liu Y, *et al.* Organic microcrystal vibronic lasers with full-spectrum tunable output beyond the Franck-Condon principle. Angew Chem Int Ed, 2018, 57: 3108–3112
20 Zhang Q, Su R, Liu X, *et al.* High-quality whispering-gallery-mode lasing from cesium lead halide perovskite nanoplatelets. Adv Funct Mater, 2016, 26: 6238–6245
21 Wang X, Shoaib M, Wang X, *et al.* High-quality in-plane aligned $CsPbX_3$ perovskite nanowire lasers with composition-dependent strong exciton–photon coupling. ACS Nano, 2018, 12: 6170–6178
22 Lawandy NM. Coherent random lasing. Nat Phys, 2010, 6: 246–248
23 Wiersma DS. The physics and applications of random lasers. Nat Phys, 2008, 4: 359–367
24 Sun TM, Wang CS, Liao CS, *et al.* Stretchable random lasers with tunable coherent loops. ACS Nano, 2015, 9: 12436–12441
25 Hu HW, Haider G, Liao YM, *et al.* Wrinkled 2D materials: a versatile platform for low-threshold stretchable random lasers. Adv Mater, 2017, 29: 1703549
26 Zhu H, Shan CX, Zhang JY, *et al.* Low-threshold electrically pumped random lasers. Adv Mater, 2010, 22: 1877–1881
27 Redding B, Choma MA, Cao H. Speckle-free laser imaging using random laser illumination. Nat Photon, 2012, 6: 355–359
28 Wang YC, Li H, Hong YH, *et al.* Flexible organometal–halide perovskite lasers for speckle reduction in imaging projection. ACS Nano, 2019, 13: 5421–5429
29 Xu FF, Li YJ, Lv Y, *et al.* Flat-panel laser displays based on liquid crystal microlaser arrays. CCS Chem, 2020, 2: 369–375
30 Lin CH, Zeng Q, Lafalce E, *et al.* Large-area lasing and multicolor perovskite quantum dot patterns. Adv Opt Mater, 2018, 6: 1800474
31 Wang K, Du Y, Liang J, *et al.* Wettability-guided screen printing of perovskite microlaser arrays for current-driven displays. Adv Mater, 2020, 32: 2001999
32 Ren Y, Zhu H, Wu Y, *et al.* Ultraviolet random laser based on a single GaN microwire. ACS Photonics, 2018, 5: 2503–2508
33 Wang Z, Meng X, Kildishev AV, *et al.* Nanolasers enabled by metallic nanoparticles: from spasers to random Lasers. Laser

Photonics Rev, 2017, 11: 1700212
34 Haider G, Lin HI, Yadav K, *et al.* A highly-efficient single segment white random laser. ACS Nano, 2018, 12: 11847–11859
35 Wang Z, Meng X, Choi SH, *et al.* Controlling random lasing with three-dimensional plasmonic nanorod metamaterials. Nano Lett, 2016, 16: 2471–2477
36 Li X, Wang Y, Sun H, *et al.* Amino-mediated anchoring perovskite quantum dots for stable and low-threshold random lasing. Adv Mater, 2017, 29: 1701185
37 Yakunin S, Protesescu L, Krieg F, *et al.* Low-threshold amplified spontaneous emission and lasing from colloidal nanocrystals of caesium lead halide perovskites. Nat Commun, 2015, 6: 8056
38 Wang Y, Li X, Song J, *et al.* All-inorganic colloidal perovskite quantum dots: a new class of lasing materials with favorable characteristics. Adv Mater, 2015, 27: 7101–7108
39 Protesescu L, Yakunin S, Bodnarchuk MI, *et al.* Nanocrystals of cesium lead halide perovskites ($CsPbX_3$, X = Cl, Br, and I): novel optoelectronic materials showing bright emission with wide color gamut. Nano Lett, 2015, 15: 3692–3696
40 Dong H, Zhang C, Liu X, *et al.* Materials chemistry and engineering in metal halide perovskite lasers. Chem Soc Rev, 2020, 49: 951–982
41 Quan LN, García de Arquer FP, Sabatini RP, *et al.* Perovskites for light emission. Adv Mater, 2018, 30: 1801996
42 Chen R, Bakti Utama MI, Peng Z, *et al.* Excitonic properties and near-infrared coherent random lasing in vertically aligned CdSe nanowires. Adv Mater, 2011, 23: 1404–1408
43 Luo Z, Chen Y, Wu ST. Wide color gamut LCD with a quantum dot backlight. Opt Express, 2013, 21: 26269–26284
44 Arsenault AC, Puzzo DP, Manners I, *et al.* Photonic-crystal full-colour displays. Nat Photon, 2007, 1: 468–472
45 Deng R, Qin F, Chen R, *et al.* Temporal full-colour tuning through non-steady-state upconversion. Nat Nanotech, 2015, 10: 237–242

Acknowledgements This work was financially supported by the Ministry of Science and Technology of China (2017YFA0204502), and the National Natural Science Foundation of China (21790364).

Author contributions Zhao YS conceived the concept and planed the project. Zhao YS supervised the research. Hou Y designed and performed the experiments and prepared the materials. Hou Y, Zhou Z, Zhang C, Tang J, Fan Y and Xu FF carried out the optical measurements. Hou Y and Zhao YS analyzed the data and wrote the paper. All authors discussed the results and commented on the manuscript.

Conflict of interest The authors declare that they have no conflict of interest.

Supplementary information Experimental details and supporting data are available in the online version of the paper.

Yue Hou obtained her BSc degree from Lanzhou University in 2016. She is currently working on her PhD degree in Professor Zhao's group at the Institute of Chemistry, Chinese Academy of Sciences (ICCAS). Her research interests are the photonic properties of micro/nanomaterials and their applications as miniaturized photonic devices.

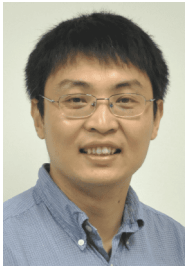

Yong Sheng Zhao received his PhD degree in 2006 at ICCAS. After that, he joined the University of California at Los Angeles (UCLA) and Northwestern University as a postdoctoral fellow. In 2009, he returned to ICCAS as a professor of chemistry. His research interests include the controllable synthesis of low-dimensional organic materials, photophysical and photochemical processes, as well as the fabrication and performance optimization of photonic/optoelectronic devices.

基于随机激光阵列的全色柔性激光显示

侯悦[1,2], 周忠豪[1], 张春焕[1], 汤济[1], 范宇晴[1,2], 徐法峰[1], 赵永生[1,2*]

摘要 柔性激光显示是下一代可穿戴设备的重要组成部分. 到目前为止, 由于缺乏能够在机械条件下稳定工作的显示面板, 柔性激光显示的发展受到了阻碍. 随机激光器得益于多重反馈的工作机制可以承受机械变形, 是实现柔性激光显示面板的理想选择. 然而, 目前缺少一种通用的制备方法将随机激光器精确排布成高度有序的像素化矩阵. 为此我们提出了一种适用于柔性显示面板的全色随机激光阵列的构建策略. 在构建的微激光像素中, 多重散射可以提供持续的光学反馈回路, 使得随机激光可以稳定出射. 在机械变形下激光的性能也可以很好地保持, 从而实现高性能的柔性激光显示面板. 我们的构建策略将为柔性激光显示和激光照明设备的发展提供有益的参考.

